1 Experiment 1

The demonstrations in?? and ?? seem to suggest that the perceived reversal of motion direction is a function not only of carrier strength of individual elements but of a spacing-dependent interaction between nearby elements. We explored this spatial interaction by examining the interactions between local and global motion as a function of both the distance betwee...n elements and the carrier strength.

1.1 Methods

Stimuli for these experiments were all presented at a fixed eccentricity of 6.7° and used a complete circle of evenly spaced elements. For each session we chose a set of carrier strengths and spacings, and collected psychometric functions for each member of the set, with the abscissa of each function being the envelope motion. As described above in ??, we used an interleaved staircase procedure to collect psychometric functions, with the staircase varying the speed of the envelope motion. There were two general types of sessions. One type was focused on the effect of spacing, and tested several spacings at a single carrier strength. chosen based on preliminary data from that subject.). Another type was focused on the effect of carrier strength, and tested a fixed set of carrier strengths (0.1, 0.2, 0.4 and 1.0), at two values of spacing. The particular values of spacing and direction content employed were selected based on preliminary sessions with that subject. There may be some adaptation when a single carrier strength or limited sets of spacings were used for an entire session. However, we find that a single model fits the both datasets adequately, so we pool the data from both types of experiments and present them together here.

1.2 Results

We first compare individual psychometric functions that illustrate the effects of spacing, carrier strength and envelope displacement. There are three qualitative effects that we wish to point out before combining them all into a unified presentation of the model.

1.2.1 Sensitivity to displacement decreases as spacing decreases

One effect of changing spacing is to change the observers' sensitivity to envelope motion. Consider the psychometric function whose domain is the envelope motion (spatial distance between stations, or Δx) and whose range is the probability of the observer responding "clockwise" to that stimulus. We find that when the spacing between elements is reduced, the slope of this function decreases. An example of this is shown in figure 1. The curves in that figure reflect an overall fit of the model described in section §??, while the points reflect the observed responses at a particular carrier strength, spacing, and direction content. The points on the graph are scaled according to the number of trials completed with

those stimulus configurations. Therefore we would expect larger points to lie closer to the model fit, while smaller points have more uncertainty and may be expected to lie farther from the model fit. In the extreme, a particular stimulus configuration might only be visited once while the staircase moves past it; these smallest points will lie on either $P(clockwise) = 1$ or 0. Since the curves plotted are overall model fits rather that fits to only the stimuli shown, we expect some degree of mismatch between model and data.

We consistently observe that reducing the spacing between elements also reduces the slope of the psychometric functions. Thus, when elements are more closely packed together, it appears to be more difficult for observers to discriminate the direction of envelope motion. Nearby elements thus interfere with the ability to discriminate changes in elements position. Note that in this experiment, reducing the spacing between elements correspondingly increases the number of elements in the scene. One might have expected that there could be pooling of envelope motion signals from separate elements, in which case we would expect that the sensitivity to envelope motion increases with additional elements on the display. We do not see this, even for the difference between two and four elements (one or two per hemifield) which should be outside the range of any crowding effects. So it appears that in this task envelope motion is not pooled, even with knowledge in the task that the motion of all elements is identical. So we also rule out the possibility that envelope motion is globally pooled among elements, at least for this task and stimuli; if pooling of envelope motion occurred, we would observe the opposite effect on the slopes of the psychometric functions.

We should also note that the values of Δx tested are substantially smaller than half the inter-element spacing, so that spatial aliasing (i.e. the wagon wheel illusion) should not explain why there is additional uncertainty in motion direction.

1.2.2 Sensitivity to carrier strength increases as spacing increases; carrier motion is repulsive at wide spacings

Observers' responses to the carrier component of the motion were in some ways more complicated then their response to the envelope motion. One feature is that carrier motion can be repulsive; weak amounts of carrier motion in one direction often caused a tendency for observers to report perceived motion in the opposite direction. Another feature is that the sensitivity to carrier motion, in these stimuli, changed as a function of the spacing between elements. Figure 2 gives an example of both these effects, using a subset of the data collected. In that figure we show psychometric functions collected at two different values of carrier strength at two different element spacings. The lower row shows data collected at the wider of the two spacings. The psychometric functions shown here show a repulsive effect of carrier motion; they intercept the $\Delta x = 0$ axis at a value less than 0.5, indicating that observers were more likely to perceive

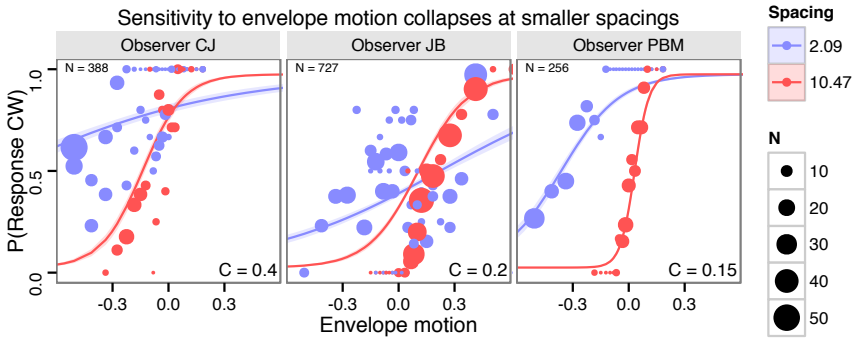

Figure 1: Effect of spacing on sensitivity to direction content. Psychometric functions of envelope motion are shown for three example subjects. For each observer two curves are shown, each at a different spacing; carrier strength is unchanged. The effect of reducing spacing is to reduce the slope of the psychometric function, indicating that nearby elements interfere with observers' ability to detect an element's change in position. Curved lines show model fits, while dots show observed data; the size of each dot corresponds to the number of trials observed by the staircase procedure at that displacement. The curves plot fits from the overall model as described in section §**??**, which was fit to a much larger set of data than is shown here (so we expect individual curves may not fit ideally to the small subset of data shown here.)

a stimulus with null envelope motion and clockwise carrier motion as actually moving counterclockwise.

Note that since this graph presents folded data, i.e., values shown here with a single value for carrier strength, which we nonetheless refer to as "clockwise," represent data collected from both that stimulus and its mirror image, and envelope motions and responses are mirrored correspondingly. So a point appearing below $P(cw) < 0.5$ in this graph indicates that the observer chose "counterclockwise" to a particular stimulus more often than they chose "counterclockwise" to that stimulus's mirror image. Thus the presentation of folded data here averages out any static biases toward one direction that an observer may have.

In fact any data appearing in the lower right quadrant of this graph shows stimuli for which carrier motion is (nominally) clockwise, envelope motion is clockwise, and yet the observer reported counterclockwise motion on average – that is, against both the carrier and envelope motions.

Moving to the graphs in the upper row, we see that the repulsive effect is no longer evident. Now nominally clockwise values of carrier strength are associated with increased rates of responding "clockwise", and increasing the carrier strength further increases the rate of clockwise responses. So the repulsion may only be active at larger spacings, or it may be present at smaller spacings while being overwhelmed by a spacing-dependent effect (see section 1.4.5) We also observe that the effect of changing carrier strength is larger when inter-element spacing is reduced. For an identical change in carrier strength, distance between the $\Delta x = 0$ intercepts for two strengths of carrier motion is much larger at the narrow spacing than at the larger spacing. Note that we would expect the distance between the points of subjective equality (the intercepts of the psychometric functions with $P(cw) = 0.5$) to be increased even of the strength of carrier motion did not change, simply because of the reduced sensitivity to envelope motion described in the previous section and apparent as a change in the slope of the psychometric functions between upper and lower rows. Since the intercepts with the vertical axis are also farther apart at smaller spacings, we conclude that the sensitivity to carrier motion has increased in addition to the decrease in sensitivity to envelope motion.

There are alternative ways to interpret the spacing-dependent change in the strength of carrier motion and the shift from repulsion to assimilation. One is as a form of center surround effect, in which the spacing-dependent interaction takes the form of repulsion between widely spaced element and obligatory summation between more closely spaced elements, as has been observed for other visual features such as orientation Mareschal et al. (2010). Another interpretation is that the repulsion is an induced-motion effect that operates independently of the spacing-dependent effect and the increase in sensitivity to carrier motion depends on a sum of motion energy over the visual field (thus the number of elements is more relevant than the spacing.) We will attempt to clarify and distinguish between these interpretations in the subsequent experiment. In either case, this contrast identifies a way in which envelope motion is seen differently from carrier motion; it appears that envelope motion signals from separate objects cannot be combined in this task, while carrier motion

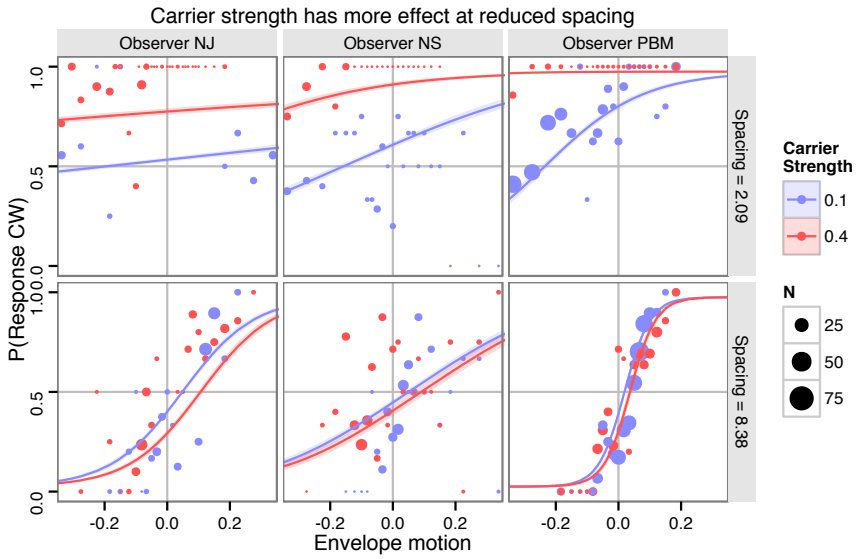

Figure 2: Reducing spacing increases the effect of carrier motion; carrier motion at large spacings is repulsive. An example subset of the data from Experiment 1 tupper row shows data taken a wide spacing while the lower row shows data taken at a narrow spacing. Each subplot shows two psychometric functions taken at two different carrier strengths. In addition to the effect of spacing on sensitivity to direction content, seen in the previous figure, this plot illustrates the changing effect of carrier strength as a function of element spacing; the does not change the intercepts of the psychometric functions very much, while the same change at narrow spacing produces a much greater change in the proportion of observers' responses toward one direction. We also see that weaker carrier strengths are repulsive when targets at wide spacings; In the bottom row, curves intersect the $\Delta x = 0$ axis with the observer reporting clockwise motion with probability less than 0.5 (with the convention that carrier motion is always taken to be clockwise.)

does appear to combine between adjacent objects.

1.3 Model and data overview and visualizations

Our experiment relates three parameters – carrier strength, envelope motion and spacing – to a fourth variable, the motion perceived by the observer. At this point, having given examples illustrating some of the effects that a model should capture, we attempt to present an overview both of the entire dataset, and how the model fits that data. Afterwards we will examine particular features of the model and evaluate their fit to the data.

This experiment observed the effect on perceived motion of three stimulus parameters (spacing, envelope motion, and carrier strength.) We can visualize those variables as forming a three-dimensional configuration space. As a function of these three variables, we model the proportion of responses on one direction or the other.

These graphs display the models fitted to each subject's data, while showing locations at which data was sampled. The model has three primary variables (spacing, envelope motion, and carrier strength) which we are concerned with; these variables can be considered to form a three-dimensional stimulus configuration space. The combination of these three variables determines the likelihood with which the observer will respond "clockwise" or "counterclockwise" to the given stimulus. Here we show the model's predictions over four planar sections through this three-dimensional space.

1.3.1 Model figure construction

Figure 3 shows a perspective view of the three stimulus parameters varied in this experiment, as a three-dimensional space with four intersecting planar sections shown. Data from one observer is shown; the complete set of illustrations for all observers is shown in an appendix. The color scale maps response probabilities to luminance with darker and more saturated hues mapped to response probabilities that are further from 0.5. Additionally color is mapped to the sign of the response probability, with blue shades representing points where the modeled observer tended to respond counterclockwise (that is, against the direction of carrier motion) and red hues representing points where the response favors the direction of carrier motion. Four planes are illustrated within this space. These planes are the same as the subplots shown in the lower half of the figure.

Each panel in figure 4 shows the model's predictions as a function of two of the three variables, leaving the other fixed; the value of the fixed variable is noted in the upper right corner of each panel. From upper right counterclockwise, we show how (a) model responses vary as a function of spacing and carrier strength, for stimuli with zero envelope motion, (b) as a function of spacing and envelope movement, for stimuli with zero carrier motion, (c) as a function of envelope motion and carrier strength, for stimuli with a fixed, narrower spacing, and (d) as a function of envelope motion and carrier strength (similarly to (c)), for stimuli with a fixed, wider spacing.

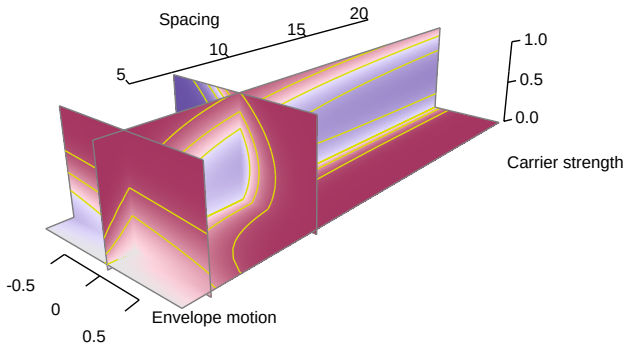

Figure 3: A three-dimensional representation of the model fit for one observer (NJ). Axes correspond to the three stimulus parameters varied in this experiment: inter-element spacing S in degrees, envelope motion Δx, in degrees per step, and carrier strength C, are placed along three axes. The color scale indicates the probability of responding clockwise predicted by our model. Four sections through the notionally three-dimensional space are shown, and correspond to the four panels in figure 4. Red shades indicate stimuli for which the model predicts responses that agree with the direction of carrier motion (whose strength is plotted on the vertical axis) and blue shades indicate stimuli where the model's predicts responses that disagree with the direction of carrier motion. In both cases the luminance depends the difference between the response probability and 0.5, with response probabilities further from 0.5 are colored darker and more saturated. Yellow contour lines are placed at response probabilities of 0.1, 0.3, 0.5, 0.7 and 0.9.

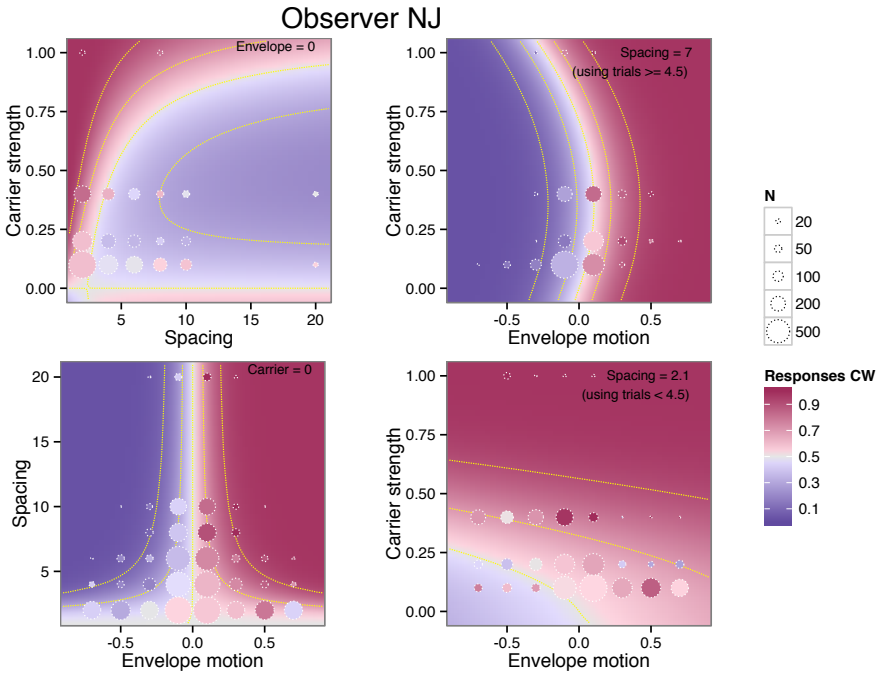

Figure 4: Data and model responses for observer NJ. The four plots shown correspond to the four planes shown in figure 3; color scale and contour line placement are the same. Circles represent observers' recorded responses near a particular stimulus. The shading of each circle depends on the residual between the recorded responses and the model prediction for that set of stimuli; an identical shade inside the circle as outside indicates no residual. Each circle represents the subset of trials falling nearest that point. Upper left: we plot the response probability as a function of carrier strength and spacing, with envelope motion fixed to zero. Circles collect trials with all envelope motions. Lower left: we show the response probability as a function of envelope motion and spacing, for stimuli with no carrier strength (i.e. counterphase) Upper right and lower right: We plot the fitted model response as a function of carrier spacing and strength, for two different values of spacing (indicated;) the upper left plot is taken at a relatively wider spacing while the lower left plot is taken at a relatively narrower spacing. In plotting the shaded circles indicating residuals, the upper left plot shows that the Trials are divided between these plots; the upper left plot computes residuals from trials that used a wider spacing and the lower left plot shows residuals from trials that had a narrower spacing (as indicated). Both plots on the left use all trials in computing residuals.

Figure 4 also depicts the observer's responses. Circles plotted have shading determined by the observer's recorded responses, and each circle's area corresponds to the number of trials represented by that circle. The shading within the circle represents an average of the observers' responses at the stimulus parameters where the circle is drawn. Any difference between the shading inside the circle and that of the background indicates a residual between the model and the subset of observed data falling closest to that circle. The area of the circles scales in proportion to the number of trials represented.

Note that the shading within each circle is not simply the arithmetic mean of observers' responses, but is based on the difference between the data and model fit; we need to base the plot on residuals rather than the mean for a few reasons. One is that the actual stimulus parameters of the trials are scattered through the 3-D space outlined in the upper figure, and the underlying response probability depends on all three dimensions. Each circle collects the subset of trials that lie closest to it, but the underlying response probabilities we are trying to model still differ over that subset. In the upper left figure the points collected under one circle at a particular value of displacement can take any value in the unseen dimension (envelope motion); and with reverence to the other plots we see that at a particular spacing and carrier strength, the response is expected to vary as a function of envelope motion. Observing a response probability of 0.5 for some particular stimulus, means different things depending on if the model predicts 0.2 (the model undershoots) or 0.8 (the model overshoots); Therefore we base the plot on the difference between model and observation rather than taking the mean of the raw observations.

Another reason is that the data are not evenly sampled throughout the stimulus configuration space. For example, in the upper left plot, each circle represents a number of trials that occur over a number of different envelope motions; because a staircase procedure was used, the set of envelope motion values that was collected differs for each circle. If each staircase procedure converged well, using the arithmetic mean would plot a probability close to 0.5 for all circles in the upper left graph; but this would not be useful for assessing the model fit or the behavior of the observer.

The shading used inside the circles should be interpretable against the background, so we compute the shade by asking "what response probability for the configuration at which the circle is centered would give the same Pearson residual as we actually observe for these trials at this sample size." If the model fits exactly, the interior of each circle will match the exterior. If the shade differs, it indicates that we observed more clockwise or counterclockwise responses than the model predicts, depending on the direction of the difference.

1.3.2 Model figure

The four plots in figure 4 illustrate each of the effects with have discussed with respect to carrier strength, direction content, and spacing. The lower left plot shows how the observer's response varies for stimuli with no carrier motion (i.e. with all elements flickering in counterphase.) The horizontal axis measures the

degree of carrier motion used in the stimulus, while the vertical axis measures the inter-element spacing. When there is no carrier motion, observers tend to report clockwise apparent motion for envelope motions that are clockwise, and vice versa. This is reflected by the right half of the graph taking values > 0.5(in red) and the left half of the graph taking values less than 0.5 (in blue). (Because the data are folded, this graph only shows circles where $\Delta x > 0$.)

The effect captured by the lower left plot is that sensitivity to envelope motion (graphically, how fast the transition is, in the horizontal direction, from deep blue to deep red) changes as a function of spacing. In our model this spacing-dependent sensitivity is described by the function $\beta_{\Delta x}(S)$ and is controlled by the sensitivity parameter $\beta_0$and the "critical spacing" parameter S_C. The data that is observed, whose residuals are plotted in circles tend to concur with this behavior. Note that at smaller spacings, data has been collected over a wider range of envelope motions than at the largest spacings. This is a result of using the interleaved staircase procedure which will step over a wider range when the sensitivity is larger. Note that even at the smallest spacings most data has been collected with envelope step sizes quite a bit less than 0.5; so that inherent ambiguity with forming correspondences between element appearances (i.e. the wagon wheel illusion) should not contribute to the lessening of sensitivity.

While sensitivity to envelope motion decreases when spacing is reduced, the sensitivity to carrier motion typically increases. The combination of the two effects can be seen in comparing the two graphs at the right of figure 4. When spacing is relatively wide, as in the upper right panel, the gradient of the decision function is steeper along the axis of envelope motion, and the model is relatively insensitive to carrier strength. In the lower left graph the situation has reversed. With reference to the space shown in figure 3 we can imagine the surface formed by the set of stimuli for which observers equivocate; it takes a 90 degree twist as spacing decreases. perception of motion is driven by envelope motion at wider spacings but by the carrier when spacing is narrow.

Another effect is included in the model which depends on the strength of carrier motion. This is the repulsion effect characterized by $M_i(C)$. Its effect is to make weak carrier motions slightly repulsive; that is, adding a moderate amount of carrier motion that is clockwise tends to make observers report more counterclockwise apparent motion. This effect is nonlinear as a function of carrier strength; carrier strengths less than 0.4 generally cause repulsion but as the carrier strength approaches 1 again, directed carrier motion instead causes observers to report apparent motion in the same direction.

In the upper right figure, we have plotted response probabilities as a function of envelope motion and carrier strength, for a relatively wide spacing. Consider starting at the point (0,0) where the response probability is 0.5. As you travel up the graph, corresponding to adding carrier motion, the modeled response probabilities drop below 0.5, exhibiting repulsion. Increasing the carrier motion further we find that the repulsion reverses and the observer now reports motion in the direction of the carrier.

The upper left graph shows the combined effects of both the nonlinear repul-

sion and spacing-dependent summation effects. Here we have fixed the envelope motion to zero. At relatively wide spacings, we see that there is much repulsion, indicated by mostly blue colors on the right side of the graph. However the repulsion effect disappears at the strongest carrier strengths (at the top of the graph) and at narrower spacings. Both the repulsion at weak carrier strengths and its reversal at at high carrier strengths occurred for most observers in our sample.

As modeled this repulsion effect is independent of both the number of elements on the display and the spacing between them. We attempted changing or adding similarly formulated terms that were dependent on element number and on spacing, but these did not result in better fits as assessed by the AIC measure (Akaike, 1974).

Similar patterns of behavior are found for most observers. The set of plots for all observers who participated in this experiment is included in an appendix (section §**??**.)

It is worth discussing the areas where the model does not do as good of a job in reproducing observers' data. We often find that the repulsion measured at a carrier strength of 0.2 is stronger than the model fit (and the repulsion at 0.4 is weaker.) So the functional parameterization we have chosen for $M_i(C)$ might need to be improved, however we do not have a mechanism in mind that would inspire a better parameterization.

Another area where the model does not fully capture the observers' behavior is that their responses at smaller spacing are more variable at than the model would predict. This is visible to some extent in the raw data plotted in figure 1; rather than the smooth psychometric function that is fit to the data. the data points have more scatter or oscillation around the fit. This is also visible in the bottom row of circles in the lower left panel of figure 4, where the differences between model and observed data are more apparent. It may be significant that the stimuli are narrowband with a relatively well defined spatial period to the carrier. This may produce spatial aliasing; different speeds of envelope motion (corresponding to different lengths of the spatial step between successive appearances of the Gabor-like element) may cause peaks and troughs to line up. When the locations of the envelope are obscured by the presence of flankers, the visual system may resort to aligning first-order peaks and troughs rather than second-order envelope locations. Some individual psychometric functions for some observers are suggestive of an oscillation on the order of the spatial period of the carrier, but we have not been successful in improving the model fit by adding a term accounting for this. Subjectively, the experience of stimuli at high density is "confusing" and observers report, e.g. that different motions overlap, or that the appearance of the stimulus changes as a function of attention; observers' responses may vary according to a choice of strategy or attending to different aspects of the stimulus.

1.4 Model components and measurement of effects

We have described three separate effects: a reduction in the sensitivity to envelope motion as inter-element spacings reduce, a concurrent increase in the sensitivity to carrier strength, and an independent repulsion that depends nonlinearly on the carrier strength but not on the spacing. Since the effects involve mutually overlapping stimulus parameters, comparisons of behavior along any one dimension involve overlapping effects, which makes it less obvious which effect is responsible for which features of behavior. Additionally we observe a relatively large amount of individual variation in observer's behavior – I have configured a demonstration stimulus with both carrier and envelope motion moderately clockwise, which appeared clearly clockwise to me, while a naïve observer viewing the same stimulus at the same time, it was clearly counterclockwise. In earlier experiments, some observers perceive motion to reverse when spacing is changed holding other stimulus parameters constant, but we were not able to find a stimulus configuration that produced the reversal consistently across observers. We suspect that multiple motion sensing mechanisms are responsible for observer's behavior in this experiment; when multiple mechanisms are involved, the relative strengths of these mechanisms vary between observers, with qualitatively different effects.

We would like to distill out the distinct effects we see each into its own measurement. This will help us evaluate and provide some justification for the particular functional forms that have chosen in our model, as well as show how individual effects are consistent across observers.

1.4.1 Lack of pooling across large distances

We motivated the description of our model (section §**??**) by considering that the observer attends a single element of the display; other elements were taken to be ignored as best the observer is able, though they exert an influence via effects like crowding or summation depending on distance. However, in our task the stimulus is composed of identical, identically moving elements. Therefore in principle, it is not necessary that a subject isolate any particular element to arrive at a veridical perception of envelope motion; any element will do the same job. When distinct objects move concurrently, one can perceive the motion as of a larger element of which the distinct components are features, as in Ternus displays (e.g. Boi et al., 2009) or as when motion is consistent with the motion of a rigid body (e.g. Anstis and Kim, 2011.) In our displays, the motion of all elements in the display is consistent with that of a wheel rotating around the fixation point, at least if you consider envelope and carrier motion separately. Knowing this, an ideal observer could in principle pool multiple envelope position signals in order to improve sensitivity to envelope motion. If that is the case than the sensitivity to envelope motion (i.e. the slope of the psychometric function relating envelope motion to response probability) should increase when additional, coherently-moving elements are added to the display, as long as targets remain widely separated enough to avoid crowding.

For 9 of the observers who participated in this experiment, we measured psychometric functions with both 2 and 4 elements on the display (at an eccentricity of 6.67°, corresponding to spacings of 20.9° and 10.5° around the circle.) These spacings should be large enough to escape crowding effects. To assess the presence or absence of pooling at large distances we compared observers' sensitivities to envelope displacement at 2 and 4 elements using a logistic regression model formulated as

$$\Pr\left(\text{clockwise} \mid \Delta x, C, n\right) = \text{logit}\left(\beta_n \Delta_x + k_{|C|,n} C + b\right)$$

where the slope of the psychometric function corresponds to β_n and a separate intercept is used for each absolute value of direction content and element number. Using a treatment contrast for β_n, we asked how sensitivities changed as a function of element number. For 6 of the observers, the sensitivity coefficient decreased at 4 elements as compared to 2; for the remaining 3 it increased. However, any change only reached a significance level of $p < 0.05$ for only one observer (whose sensitivity decreased as element number changed from 2 to 4.) The subset of data considered here comprises 5561 trials. We conclude that there is not pooling of envelope motion data between separate objects in this experiment.

1.4.2 With shorter distances between elements, sensitivity to envelope motion declines.

A central feature of our model as illustrated on **??** is that we expect the sensitivity to envelope motion to decline as spacing between elements declines, i.e. there is a crowding effect on envelope motion. To illustrate this effect we derive a measurement of the effect size as a function of spacing, disentangled from other effects (carrier motion summation and repulsion.) We do this by removing the parameterization of $\beta_{\Delta x}(S)$ from the model and instead including a separate coefficient $\beta^S_{\Delta x}$ for each distinct value of spacing tested, forming a modified model. The fitted values of these coefficients constitute a measurement of the sensitivity to displacement as a function of spacing. The other components of the model (repulsion and carrier motion summation) remain included.

Examples of this measurement are shown in figure 5 for three observers (the entire set is shown in **??**) The measurement we obtain for sensitivity to displacement here is somewhat noisy, but we can see that the separately measured sensitivities generally approach zero as spacing approaches zero. As we discussed in section 1.4.1, as spacings become large there is no general trend for sensitivities to further increase. So both general features we chose for our parameterization of $\beta_{\Delta x}(S)$ (an asymptote at large spacings, and collapses to zero at small spacings) are consistent with the data. As a side note, we see that for observer PBM (an author) the sensitivities are much larger that for other subjects, while still showing the same kind of collapse at narrow spacings. We attribute this to overtraining relative to the naïve observers.

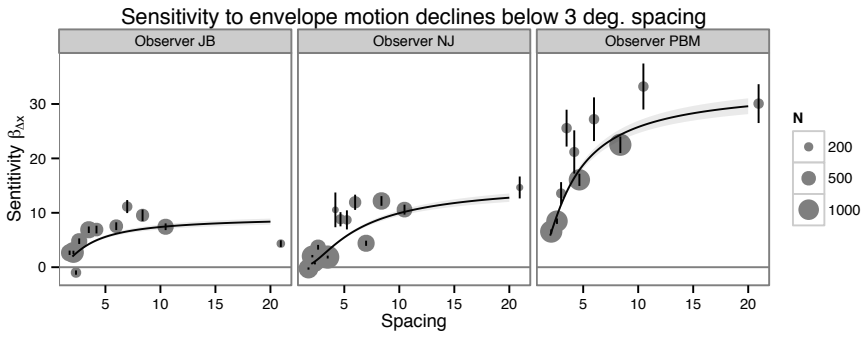

Figure 5: Sensitivity to displacement collapses as spacing decreases. In each subplot, the horizontal axis denotes spacing, while the vertical axis measures sensitivity to direction content (corresponding to the slopes of the psychometric functions shown in figure 1. Data points are obtained by re-fitting the model while allowing sensitivity to vary freely for each value of spacing, while other aspects of the model are unmodified. The size of the data points is scaled according to the number of trials underlying its measurement; vertical bars show the standard error obtained from the measurement. The vertical axis is a sensitivity measure (corresponding to the the change in log-likelihood of answering "clockwise" to a stimulus when changing Δx by 1°.) Curves show the prediction of our model fitted to the same data $\beta_{\Delta x}(S)$, as a function of spacing S. Three observers are shown here; the complete set is shown in figure **??**.

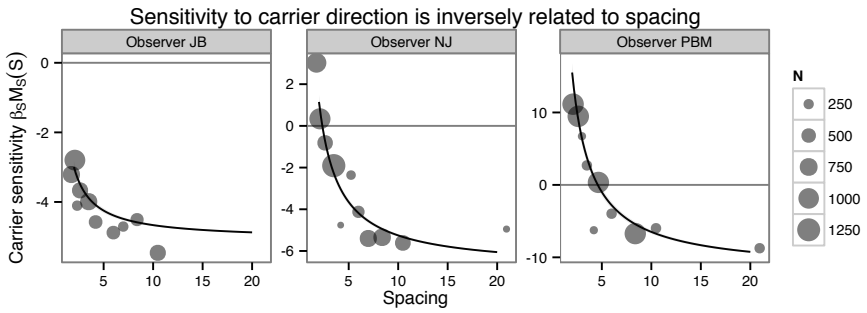

Figure 6: The sensitivity to carrier direction content increases at smaller spacings. The horizontal axis shows how the model coefficient corresponding to carrier sensitivity $M_s(s)$ (which corresponds to the distance between y-intercepts of psychometric functions of different carrier strengths, as seen in figure 2) varies as a function of spacing. Individually plotted points are obtained by letting this coefficient vary freely; curves indicate model predictions. Because the sensitivity and amount of repulsion vary between observers, each panel has a different scale on the vertical axis; the gray horizontal line indicates a sensitivity of 0, which marks the boundary between summation and repulsion. Three observers are shown here; the complete set is shown in figure **??**.

1.4.3 At shorter distances, carrier motion summates, causing an increase in sensitivity to carrier direction content.

While the sensitivity to envelope motion decreases as flanking elements are brought closer, the sensitivity to carrier motion increases at the same time. We illustrate this using the same technique as the last section, by dropping the term $M_s(S)$ and including a term $\beta_S C$ for each distinct value of spacing. We also remove the repulsive term $\beta_{I_a} C$ (as it is proportional to carrier strength and thus linearly dependent with the new $\beta_S C$ terms.) The other components of the model remain, including the nonlinear component of repulsion $\beta_{I_b} C\,|C|$, and are fitted in parallel. The units of the coefficient β_S are interpretable as the change in log-odds of responding "clockwise" when the carrier strength makes a change from 0 to 1 (ignoring the nonlinearity for the moment.) We show the results of this in figure 6. We generally find a good fit where the sensitivity to carrier strength is inversely proportional to the element spacing (or, equivalently, proportional to the number of elements) plus a constant offset.

1.4.4 At longer spacing, weak carrier direction content repels direction judgments.

Another phenomenon is visible in figure 6; first, there appears to be a constant offset to the sensitivity to carrier motion; that is, the carrier sensitivity approach some nonzero value at large spacings. This offset is generally negative; this is the repulsion effect we pointed out in section 1.2.2 In our model this is accounted for by the coefficient $\beta_{I_a} C$. When elements are widely spaced, the response to carrier motion is then dominated by the repulsion term rather than the spacing-dependent assimilation term. Interestingly, while the assimilation seemed to be simply inversely related to the spacing, the repulsion effect appears to be independent of the spacing between elements (and correspondingly with the number of elements on the screen.

1.4.5 The repulsion effect is nonlinear in carrier strength.

However, we also observe that at carrier strengths approaching 1, the repulsion effect weakens and even reverses. This effect is visible in the upper edge of the upper left panel of figure 4, where repulsion at moderate values of carrier strength become assimilation again as carrier strength is further increased. The spacing-dependent assimilation effect contributes to this, but is not strong enough at wide spacings to account for the reversal. There are two characteristics of this induced motion that deserve comment. The first is that the degree of repulsion appears to be a nonlinear function of direction content. Another is that the strength of repulsion seems to be determined by the average direction content of the elements, rather than a sum over the motion energy content of all elements, This nonlinearity is captured in the model using the function $M_I(C)$.

We confirm the presence of this nonlinearity by comparing three nested models. In the null case, we consider the model without any contribution of induced motion, that is, $M_I = 0$, but otherwise identical to the full model described above in section §**??**. The second model we consider is one in which the strength of induced motion is linearly related to the direction content of the stimulus; $M_I = \beta_I C$. For this model, we found that 10 out of 11 subjects showed a significant ($p < .05$; likelihood ratio test using a χ^2 distribution with 1 degree of freedom) improvement to the model fit by adding the linear parameter. However, we additionally suspected that the induced motion effect was nonlinearly related to the direction content of the stimulus, as Murakami and Shimojo (1993) had observed that the strength of induced motion was non-monotonically related to the contrast of the inducer for some subjects. Therefore we also considered a model in which there was a second-order, odd-symmetric component to the induced motion signal; $M_I = \beta_{I_a} C + \beta_{I_b} C\,|C|$. As compared to the linear model, we found that for all 11 subjects, the fit was significantly improved by adding the second-order component, the largest p-value being $p = 2.4 \times 10^{-7}$ for subject CJ.

Additionally, while the signs of β_I in the linear model are mixed, in the second-order model, every subject with the exception of CJ has a negative value

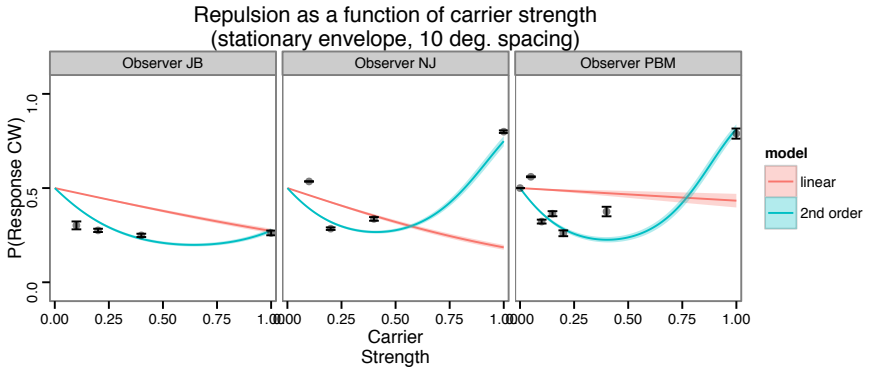

Figure 7: Effects of induced motion at wide spacing. Here we show, for each subject, the model's predicted response rates for a nominal spacing of 10°, as a function of direction content. Two shaded curves illustrate two alternative models, one where repulsion is a linear function related of carrier strength, and another where there is a second-order nonlinearity. Data points are derived from modeled data by allowing the repulsion coefficient to fit seperately for each distinct carrier strength used. The second order model obtains a better fit (see section 1.4.5.) Under this model, all but one observer (the complete set is plotted in shows a negative slope of the curve where direction content crosses zero, indicating a repulsive effect for weak direction content, while the second order coefficient weakens or reverses this effect for stronger direction contents. Three observers are shown here; the complete set is shown in figure **??**.

of β_{I_a} and a positive value of β_{I_c}, indicating that small imbalances of motion energy at wide target spacings usually lead to repulsion, but that the repulsion is proportionately weaker, or even reverses, with stronger direction content.

Figure 7 illustrates the model fits to the repulsion effect using linear and second-order models. There we show model projections for stimuli with no envelope displacement, at a fixed value of 10° element spacing, for varying values of direction content. We show fitted curves for the linear and second-order models, as well as data points corresponding to a complete model (in which the induced motion is allowed to take on a different strength for each value of C tested.) As mentioned above, for all subjects except CJ, the slope of the linear component is is negative, indicating a repulsive induced motion effect; for the same subjects the coefficient of the second-order component is positive, indicating that the repulsion proportionately weakens, or in some cases reverses, when direction content approaches $|C| = 1.0$.

References

Akaike, H. (1974). A new look at the statistical model identification. *Automatic Control, IEEE Transactions on*, 19(6):716–723.

Anstis, S. and Kim, J. (2011). Local versus global perception of ambiguous motion displays. *J Vis*, 11(3):13.

Boi, M., Öğmen, H., Krummenacher, J., Otto, T. U., and Herzog, M. H. (2009). A (fascinating) litmus test for human retino- vs. non-retinotopic processing. *J. Vis.*, 9(13):1–11.

Mareschal, I., Morgan, M. J., and Solomon, J. A. (2010). Cortical distance determines whether flankers cause crowding or the tilt illusion. *J Vis*, 10(8):13.

Murakami, I. and Shimojo, S. (1993). Motion capture changes to induced motion at higher luminance contrasts, smaller eccentricities, and larger inducer sizes. *Vision Res*, 33(15):2091–107.